Prediction of Environmental Exposures from Sources near the Ground Based on Hanford Experimental Data[1]

James J. Fuquay, Charles L. Simpson and W. Ted Hinds

Hanford Laboratories, General Electric Company, Richland, Wash.

(Manuscript received 30 October 1963, in revised form 1 April 1964)

ABSTRACT

Values of peak exposure and standard deviations of exposure distributions downwind from a continuous point source are presented for 46 Hanford ground source diffusion experiments. Exposure data are found to order in terms of atmospheric stability when plotted as a function of the travel time. The crosswind variances of the exposure distributions are expressed in terms of the travel time and the product of the standard deviation of the wind direction distribution and the mean wind speed, $\sigma_\theta \bar{u}$, in an equation resulting from G. I. Taylor's work in 1921.

Prediction methods developed from these concepts permit extrapolation of the results obtained from short releases to much longer release periods. Good agreement between predicted and observed exposure distributions is obtained from these models, using independent data.

1. Introduction

In the summer of 1959, the Green Glow Program was initiated at Hanford to obtain diffusion data out to 25.6 km from a ground source in stable atmospheres. Details of the experimental design, method of zinc sulfide plume generation, supporting meteorological instrumentation, sampling techniques, and method of sample assay have been given by Barad and Fuquay (1962a). Diffusion and meteorological data obtained in the test series have been summarized by Barad and Fuquay (1962b).

From 1960 through 1962, experimentation continued at Hanford extending the testing to periods in which the atmosphere was neutral and unstable. These tests (collectively called the Hanford 30 Series) were conducted with essentially the same experimental techniques as those of the Green Glow program. The collection of diffusion data at the outermost distances was curtailed in the 30 Series program because of manpower shortages.

The data that were obtained afford the means for a comprehensive analysis directed toward relating diffusion parameters to the meteorological measurements which were made concurrently. At this time, several results have been obtained which suggest a profitable approach in the analysis and application of experimental diffusion data. The most significant departure from most other experimental studies is that atmospheric diffusion is viewed as a time-dependent process. Significant improvement in the ordering of data, such as the peak exposure (time integrated concentration), is evidenced when these values are plotted as a function of a calculated travel time compared to results obtained by considering arc distance as the independent variable. This concept has been the basis for further analysis of the Hanford data and has led to the development of a plume growth model in which the parameters depend only on meteorological variables.

The objectives of this paper are threefold: 1) to make the Hanford data available to other investigators, 2) to present pertinent diffusion concepts which have been developed at this time, and 3) to demonstrate how these concepts may be applied in predicting diffusion.

2. The data

Of the 66 field tests that were successfully completed in the Green Glow and Hanford 30 Series programs, 46 were selected for the analysis. Twenty tests were rejected primarily because the lateral dimensions of the mean plume were not sufficiently contained within the sampling grid. Rejecting these tests eliminated the necessity for extrapolating data so that the final results are not affected by judgments of this kind. Ten of the 20 tests were set aside for later use as independent verification of prediction methods.

Tables 1, 2 and 3 are summaries of some of the meteorological and diffusion data of the 46 tests that comprise the reliable data.

Table 1 lists the test run number, date of the run and

[1] Work performed under contract No. AT(45-1)-1350 between the Atomic Energy Commission and General Electric Company.

TABLE 1. Release time, Richardson number and $\sigma_\theta \bar{u}$ for the Hanford ground source diffusion tests.

Run number	Date	Time release began	Time release ended	Ri	$\bar{u}_7$ (m sec^{-1})	σ_θ (deg)	$\sigma_\theta \bar{u}$ (rad m sec^{-1})
5	7- 8-59	2120	2150	0.097	1.7	3.6	0.107
6	7-10-59	2217	2247	0.049	3.8	8.0	0.532
7	7-13-59	2201	2231	0.119	0.9	6.6	0.104
8	7-15-59	2200	2230	0.083	2.3	4.2	0.168
9	7-16-59	2324	2354	0.112	2.5	9.5	0.415
10	7-19-59	2201	2231	0.037	5.6	4.7	0.459
13	7-24-59	2230	2300	0.078	3.3	7.7	0.442
15	7-31-59	0010	0040	0.247	1.5	18.3	0.478
17	8- 7-59	2130	2200	0.032	3.8	4.2	0.277
18	8- 9-59	2145	2215	0.031	3.9	5.7	0.386
19	8-11-59	2145	2215	0.011	5.0	7.9	0.690
21	8-14-59	2108	2138	0.067	3.8	4.5	0.296
22	8-17-59	2050	2120	0.031	4.6	5.7	0.455
23	8-18-59	2050	2120	0.018	4.8	4.3	0.360
25	8-25-59	2210	2240	0.028	4.4	7.9	0.607
26	8-28-59	2100	2130	0.036	3.7	5.1	0.329
30	2-18-60	0927	0947	(−)0.176	2.5	11.0	0.480
31	3-11-60	0955	1025	(−)0.027	3.4	8.5	0.503
32	3-15-60	0955	1025	(−)0.023	7.2	6.8	0.857
33	4-22-60	0604	0634	0.005	1.8	5.1	0.160
34	5-11-60	0522	0552	0.309	1.1	18.3	0.351
35	7-19-60	0432	0502	0.044	3.8	9.4	0.623
38	8-12-60	0510	0540	0.389	1.4	15.5	0.378
40	8-31-60	1405	1505	(−)0.117	4.1	10.5	0.750
41	9- 1-60	1657	1727	(−)0.015	6.7	4.6	0.536
42	9- 7-60	0344	0444	0.083	2.1	11.2	0.410
43	9-13-60	0522	0552	0.070	1.9	7.1	0.236
44	9-27-60	0457	0557	0.057	2.1	11.7	0.428
45	10-12-60	1248	1317	(−)0.076	6.3	12.7	1.399
46	10-18-60	0523	0614	0.086	1.6	9.5	0.266
50	4-11-61	0515	0545	0.051	3.5	8.0	0.490
51	5- 1-61	1002	1032	(−)0.229	4.8	11.3	0.946
52	5-12-61	0545	0615	(−)0.026	4.1	10.0	0.713
53	6-27-61	0550	0611	0.021	3.2	5.7	0.317
54	7-12-61	0307	0337	0.151	2.0	7.0	0.244
55	7-18-61	0356	0426	0.084	2.3	5.4	0.216
56	8- 3-61	0545	0615	0.108	0.7	10.6	0.130
57	8- 9-61	0359	0429	0.089	2.6	4.4	0.200
60	2- 9-61	0949	1019	(−)0.010	3.0	7.9	0.414
61	2-28-62	1115	1146	(−)0.085	4.2	8.2	0.601
65	7-24-62	2150	2305	0.054	4.1	10.9	0.779
66	7-25-62	2213	2313	0.074	3.0	17.4	0.912
67	7-29-62	2227	2312	0.130	1.6	8.2	0.229
68	7-30-62	2107	2152	0.048	3.9	5.5	0.374
69	7-31-62	2130	2230	0.053	4.5	13.6	1.066
70	8- 1-62	2141	2356	0.083	2.6	8.9	0.403

the times denoting the beginning and termination of the release. The Richardson number calculated from wind and temperature measurements near the source is also given. These calculations were made by a method suggested by Lettau (1957), using data collected at the 7- and 50-ft levels of the Hanford Meteorology Tower during the period of emission. The final columns contain the mean wind speed, $\bar{u}$(m sec^{-1}), the computed standard deviation of the wind direction distribution for the emission period, σ_θ(deg) and the product $\sigma_\theta \bar{u}$(rad m sec^{-1}). The speed and direction data which apply to the 7-ft level were taken from strip chart records. The standard deviation, σ_θ, was computed from its statistical definition using 20-second direction averages over the emission period.

Table 2 gives the values of the peak exposure, E_p, for each run and each arc on the Hanford grid. Exposure is often defined as the time-integrated concentration having units of gm sec m^{-3}. The peak exposure is the largest exposure value on the arc and, therefore, defines the centerline of the mean plume. The total mass of zinc sulfide, Q_t (gm), released for each test is also given.

The data presented in Table 3 are the standard deviation of the crosswind exposure distribution, $\sigma_y(m)$. This statistic, which is a measure of the lateral spread of the plume, has been calculated with the basic arc exposure data and is summarized for each run and arc distance.

3. Travel time

For this analysis, diffusion was considered to depend on the time of plume travel; values of the peak exposures and standard deviations of the observed distributions

TABLE 2. Values of peak exposure, $E_p \times 10^3$, for arcs of the Hanford grid, and Q_t.

Run no.	Arc distance (meters) 200	800	1600	3200	12,800	25,600	Q_t (gm)
5	1067	233.7	79.26	20.38	1.144	0.1495	1728
6	283	19.36	4.206	1.435	0.4599	—	1699
7	1399	214	67	7.629	0.2671	—	1699
8	1123	119.4	36.05	8.610	0.7350	—	1699
9	547.1	90.66	7.189	0.3072	0.07257	—	1215
10	462.5	34.93	10.84	2.593	0.8479	0.1869	1357
13	556.7	41.23	3.747	0.5742	—	—	2360
15	118.6	12.61	1.684	0.1909	—	—	3173
17	1171	90.64	6.198	0.5440	0.2835	—	3146
18	1042	83.62	14.79	1.846	0.7426	0.3305	3631
19	566	51.75	10.71	3.343	0.5315	0.1158	3569
21	1521	140.4	35.19	5.854	0.5523	0.5578	3600
22	1151	102	26.95	7.475	1.047	0.2892	3569
23	1096	105.1	27.15	5.135	0.4557	0.3133	3690
25	936	71.01	19.16	4.376	0.2935	0.09671	3569
26	881.8	110.1	29.73	7.387	0.5854	0.2092	3569
30	230	11.39	1.089	0.2800			728
31	308.2	16.93	4.448	1.250			1286
32	280.9	16.84	4.038	0.676			1084
33	1070	102.2	32.47	14.50			1042
34	387.2	55.44	—	7.231			886
35	143.8	11.80	4.508	1.430			279
38	396	31.10	—	1.772			571
40	581.3	21.62	4.074	0.732			1210
41	459.2	40.93	12.390	2.646			1161
42	397	38.75	11.290	2.967			643
43	209.2	42.34	—	2.639			283
44	309.6	27.16	11.03	2.460			748
45	144.8	8.735	1.754	0.3837			1240
46	838.2	124.2	31.48	8.682			972
50	478	53.15	11.390	1.976			1150
51	341.8	12.29	1.682	0.335			2015
52	647.8	47.71	10.860	3.413			2485
53	160.7	16.96	4.017	1.252			446
54	855.6	104.10	24.150	6.153			686
55	719.6	80.95	24.550	5.505			1340
56	1612	291.5	40.30	5.758			1310
57	1247.01	167.80	50.220	9.114			1410
60	725.5	67.24	13.350	6.531			1946
61	589.4	10.17	3.448	1.393			2518
65	189.3	18.60	4.749	0.895	0.1194	—	740
66	361	33.82	8.589	2.387	0.1863	—	1426
67	303.8	29.94	9.277	2.649	—	—	467
68	237.6	24.08	7.557	1.914	—	—	455
69	305	22.47	6.156	2.104	0.2557	—	1241
70	390.7	39.03	12.760	3.968	0.2068	—	911

were plotted against time rather than distance. The travel time concept is not new. Many of the classical studies of atmospheric diffusion have led to models with time as the independent variable. Sutton (1953), in his book, reviewed the works of G. I. Taylor, including an example of this approach and using Lagrangian considerations. There is thus a problem introduced in defining the travel time for experiments with measurements made in a fixed reference frame. In this study, it was determined simply by dividing the distance at which the sample was obtained by the mean wind speed at the source at the height of release, $x/\bar{u}$.

The dependence of diffusion on stability is more marked when the data are plotted against time than when the data are plotted against distance. Both time and distance relationships have been investigated. Peak exposure values which have been normalized for the wind speed and source strength stratify well in terms of meteorological parameters by using the time concept. Much of the order is lost when these data are plotted against travel distance, making it difficult to evaluate the effects of meteorological variations. The differences that can result from these two approaches are emphasized here with an example.

Data from three runs are plotted against distance in Fig. 1 and against the calculated travel time in Fig. 2. The ordinates are normalized peak exposure, $E_p\bar{u}/Q_T$ (m^{-2}). Because the most significant difference between the runs is the stability of the atmosphere associated with them, it is essential that this effect be evident in the analysis if useful prediction models are to be derived. The relationships shown in Fig. 1 are not stratified according to stability. Contrary to accepted fundamentals, the exposure data for the very stable

TABLE 3. Observed values of σ_y (meters) for arcs of the Hanford grid.

Run no.	Arc distance (meters) 200	800	1600	3200	12,800	25,600
5	12	34	64	159	715	1907
6*	34	127	202	274	527	—
7	37	146	215	301	618	—
8	15	70	161	244	460	—
9	29	108	—	312	1503	1657
10	18	56	94	166	250	1019
13	29	85	—	226	782	—
15*	—	186	—	474	603	1434
17	17	56	—	261	505	862
18	15	61	146	345	380	2100
19	28	98	182	310	594	1600
21	16	44	89	217	413	996
22	17	51	90	145	281	1054
23	17	47	86	171	860	—
25*	31	88	136	175	891	1827
26	16	41	70	122	451	1523
30	26	76	—	257	—	—
31	22	81	144	410	—	—
32	25	85	147	240	—	—
33	14	43	64	89	—	—
34*	55	201	—	326	—	—
35*	26	100	154	186	—	—
38*	43	191	—	973	—	—
40	27	84	163	325	—	—
41	16	46	80	151	—	—
42*	34	138	285	625	—	—
43	21	71	—	211	—	—
44*	46	167	300	518	—	—
45	36	146	268	427	—	—
46	27	80	—	278	—	—
50	24	88	186	460	—	—
51	35	137	187	534	—	—
52	28	75	111	178	—	—
53	17	46	90	160	—	—
54*	21	77	144	330	—	—
55	18	61	121	299	—	—
56*	36	126	295	742	—	—
57	13	32	54	111	—	—
60	19	58	90	135	—	—
61	25	87	134	503	—	—
65	40	158	314	588	1001	—
66*	55	232	453	835	1832	—
67	34	—	268	381	—	—
68	21	65	102	127	—	—
69	41	157	278	446	923	—
70	28	99	171	229	1280	—

* Bimodal or multi-modal.

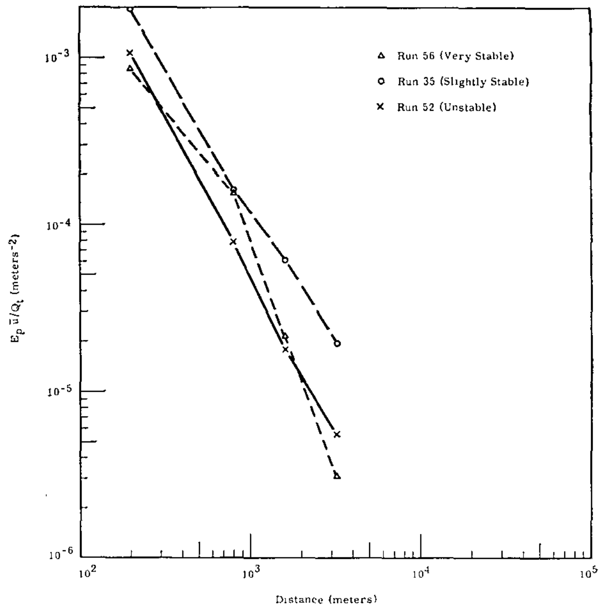

FIG. 1. Normalized peak exposure, $E_q\bar{u}/Q_T$, *vs.* distance for diffusion tests with differing conditions of atmospheric stability.

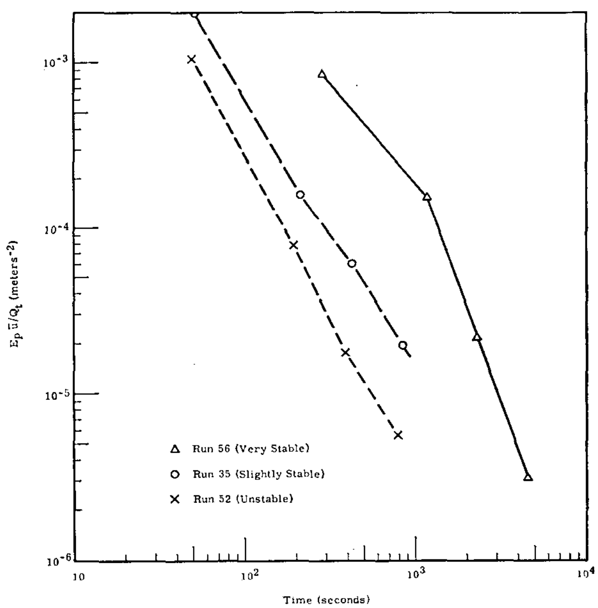

FIG. 2. Normalized peak exposure, $E_p\bar{u}/Q_T$, *vs.* time for diffusion test with differing conditions of atmospheric stability.

run are less at all distances than those for the slightly stable run. Furthermore, at 200 and 3200 meters, the stable data lie below those associated with instability. In contrast, Fig. 2 shows the same data plotted as a function of the travel time. For any given travel time, the very stable curve yields a higher exposure value than that of the slightly stable curve, which in turn is higher than that of the unstable curve.

These data were selected from the sample to demonstrate as dramatically as possible the differences in the time and distance concepts. In most cases, the effects are not so pronounced as shown, but are still evident, and there is no doubt that the stability dependence can best be identified for all of the data when travel time is taken as the independent invariable.

4. Lateral growth

Taylor (1921) identified the mean turbulent eddy energy as the significant meteorological parameter determining dispersion in the atmosphere. Assuming that the autocorrelation of eddy motions decreased exponentially with time, Taylor showed that the variance of the diffusing matter was expressed as

$$\sigma^2 = At - A\alpha + A\alpha e^{-t/\alpha}. \quad (1)$$

σ^2 is the distribution variance, t is the travel time, and A and α are parameters that determine the shape of the autocorrelation function. For lateral growth, the ratio A/α is equivalent to twice the mean lateral eddy energy, $2\overline{v'^2}$. The evaluation of $\overline{v'^2}$ would thus permit the solution of Eq. (1). A problem arises, through, in that $\overline{v'^2}$ is a Lagrangian statistic whereas meteorological measurements are made at fixed locations, making it necessary to approximate $\overline{v'^2}$ from the wind data which are readily available.

Let $\bar{u}$ be the mean wind velocity with direction $\theta=0$. Let V be an instantaneous wind at angle θ' from $\bar{u}$ with components u along $\bar{u}$ and v perpendicular to $\bar{u}$. Then $v=\bar{u}\tan\theta'$. If θ' is assumed sufficiently small, $\tan\theta'\cong\theta'$, so

$$\bar{v}+v'=(\bar{u}+u')\theta'+u'\theta'. \tag{2}$$

Squaring Eq. (2) and averaging over a span of time yields, since $\bar{v}$ is zero,

$$\overline{v'^2}=u^2\overline{\theta'^2}+2\bar{u}\overline{u'\theta'^2}+\overline{(u'\theta')^2}. \tag{3}$$

For practical purposes, Eq. 3 must be simplified; it is here assumed that the two correlation terms in (3) are small compared to $u^2\theta'^2$, and that $u=V$, so that to a first approximation,

$$v'^2=(\sigma_\theta\bar{u})^2. \tag{4}$$

Eq. (4) shows that the parameter of interest for determining σ_y is $\sigma_\theta\bar{u}$ not σ_θ alone. The results obtained in comparing the two parameters using the experimental data leave no doubt that $\sigma_\theta\bar{u}$ is superior to σ_θ as a predictor. In Fig. 3, the ratio σ_y/σ_θ is plotted against the travel time. Fig. 4 shows the ratio $\sigma_y/\sigma_\theta\bar{u}$ as a function of the travel time. The scatter of the data in Fig. 3 has been significantly reduced in Fig. 4 by simply accounting for the mean wind speed. The data points are further indentified according to the atmospheric stability as measured by the Richardson's number. The legends are included in the figures. The effect of stability on lateral growth of the plume appears to be small.

That Taylor's model was appropriate for representing the experimental data was initially suggested from the results shown in Fig. 5. The σ_y data in the plot are from only those runs in which the crosswind exposure distribution was bell-shaped. The runs which are not used are identified in Table 3 by an asterisk. The data were subdivided into groups specified by intervals of $\sigma_\theta\bar{u}$ and averaged. The data points in Fig. 5 are, therefore, the average σ_y values for the interval of $\sigma_\theta\bar{u}$ shown. The lines drawn through the data have a slope near unity at small t and appear to approach a slope of one-half at large values of t. These are the limiting values for Eq. (1).

The solution of (1) is shown in Fig. 6, where the parameters A and α have been determined from the experimental data. A rough estimate of A was readily obtained by solving the equation at large t where the constant and exponential terms are small relative to the first term. α was then estimated from the ratio $A/2(\sigma_\theta\bar{u})^2$. From these rough estimates, adjustments were made to obtain a good fit to the test data by trial and error attempts, which resulted in the following relations:

$$A=13+232.5\sigma_\theta\bar{u}$$
$$\alpha=\frac{A}{2(\sigma_\theta\bar{u})^2}. \tag{5}$$

5. Exposure

The travel time dependence of the peak exposure normalized to the source strength and the wind speed is shown in Fig. 7. The experimental data have again been divided into groups which have been jointly specified by the Richardson number, Ri, and the wind variability $\sigma_\theta\bar{u}$. The solid lines are the average exposures for the groups. The hatched areas define the limits and include all the data from which the averages were derived. The intervals of Ri and $\sigma_\theta\bar{u}$ that apply to these areas are noted.

Stratification of exposure data in terms of stability parameters is a common procedure in the analysis of experimental data. Although the identification of the stability effect has led to the development of useful prediction schemes, the range of exposures which are observed for a given stability category is still quite large. This range has been reduced by further stratification of the data with the parameter $\sigma_\theta u$. Thus, in a given stability category, the wide and narrow plumes have been separated. This effect is evident in both the stable and unstable curves in Fig. 7. The averages and limits in the figure show the extent of the data in each category. The limits would necessarily be much larger if Ri were the only criterion for stratification.

6. Prediction

The means for predicting exposure distributions have been presented. σ_y can be calculated from Eq. (1) or determined directly from Figs. 5 or 6, if $\sigma_\theta\bar{u}$ is known. The normalized peak exposure is obtained from Fig. 7 by selecting the curve appropriate for the values of Ri and $\sigma_\theta\bar{u}$, which must have been calculated. The exposure distribution for any travel time can be readily calculated with the additional assumption that distribution within the plume is normal.

In applied problems, the assumption that crosswind exposures are normally distributed is often not valid. Trends and shifts in wind direction during the period of emission will result in skewed and multimodal exposure distributions downwind. A simple method for handling these situations has been successfully tested at Hanford.

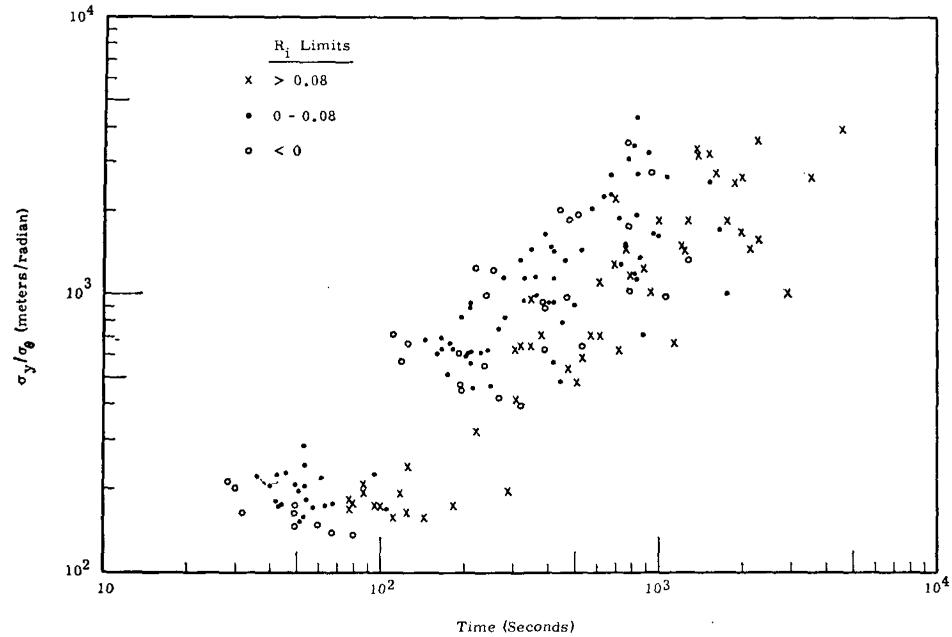

FIG. 3. Ratio of plume standard deviation to the product of wind tests with differing conditions of atmospheric stability.

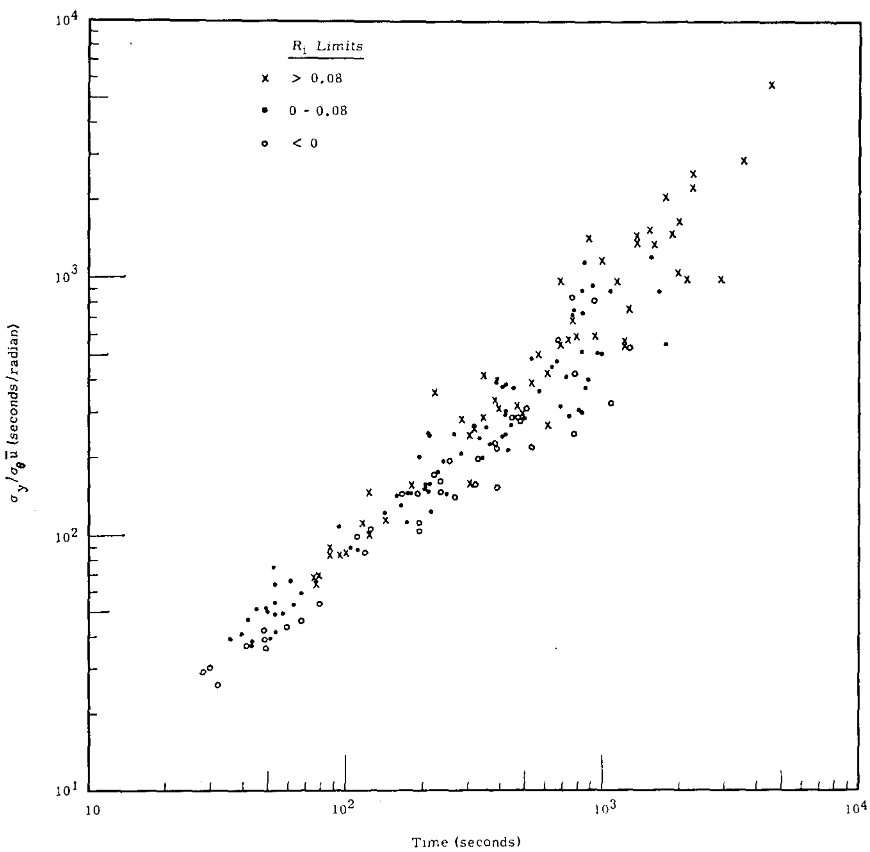

FIG. 4. Ratio of plume standard deviation to wind azimuth standard deviation times mean wind speed, $\sigma_y/\sigma_\theta\bar{u}$, *vs.* time.

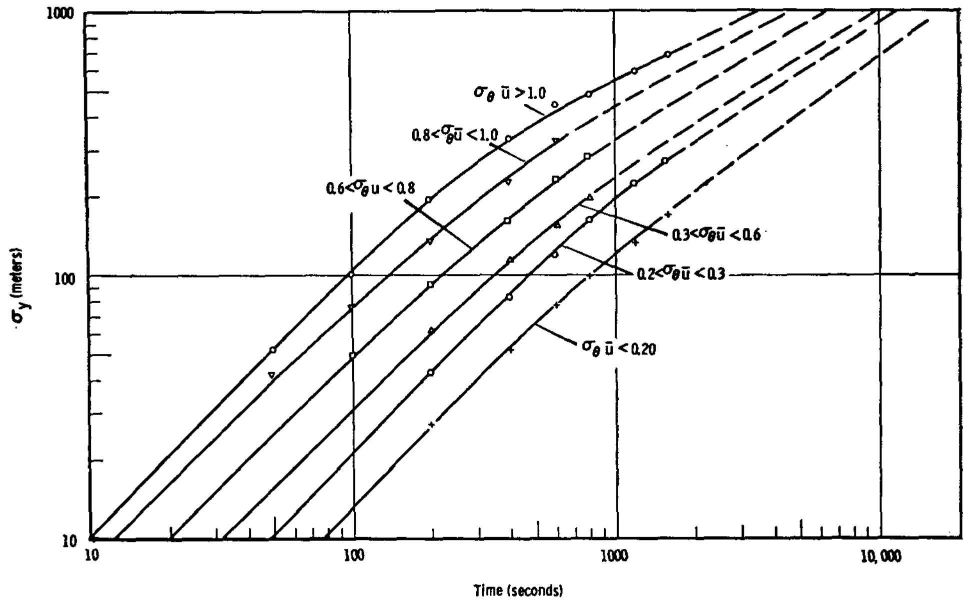

FIG. 5. Crosswind plume standard deviation, σ_y, as a function of time and $\sigma_\theta \bar{u}$.

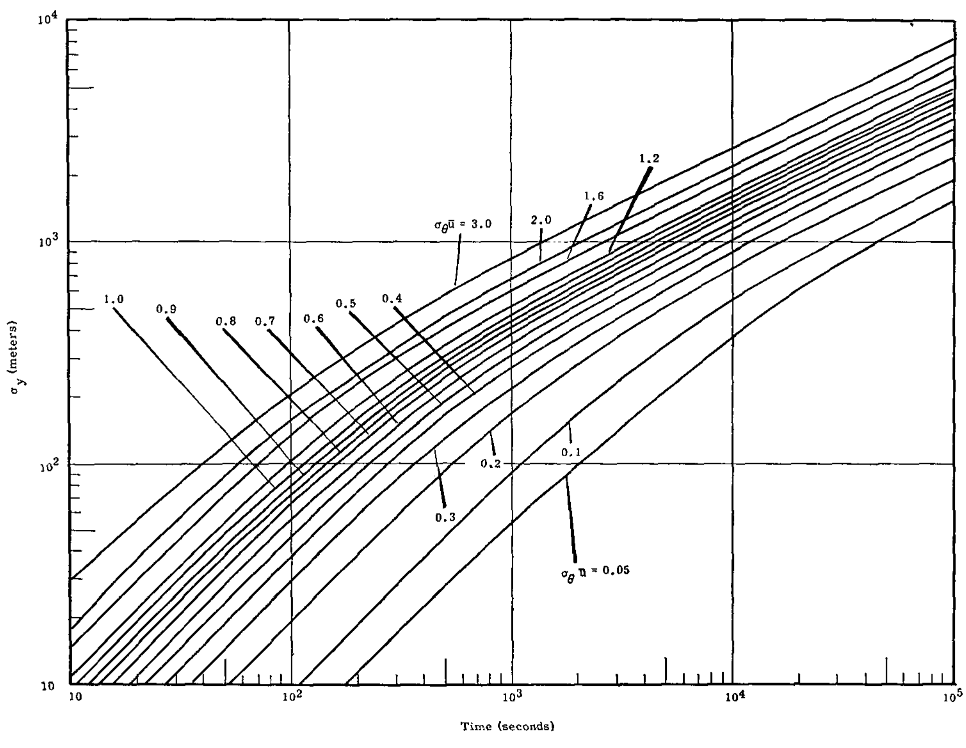

FIG. 6. Standard deviation of plume width as a function of travel time and wind variability.

When trends and shifts in wind direction are observed during the emission period, it is necessary to subdivide that period so that the frequency distribution of the wind directions within each interval is bell-shaped. A long release may thus be considered as two or more successive shorter releases, each apportioned its share of the source strength, Q, and each centered on its mean wind direction, $\bar{\theta}$. Because the intervals are chosen so that the wind distribution is bell-shaped, there is reasonable assurance that assuming the resulting

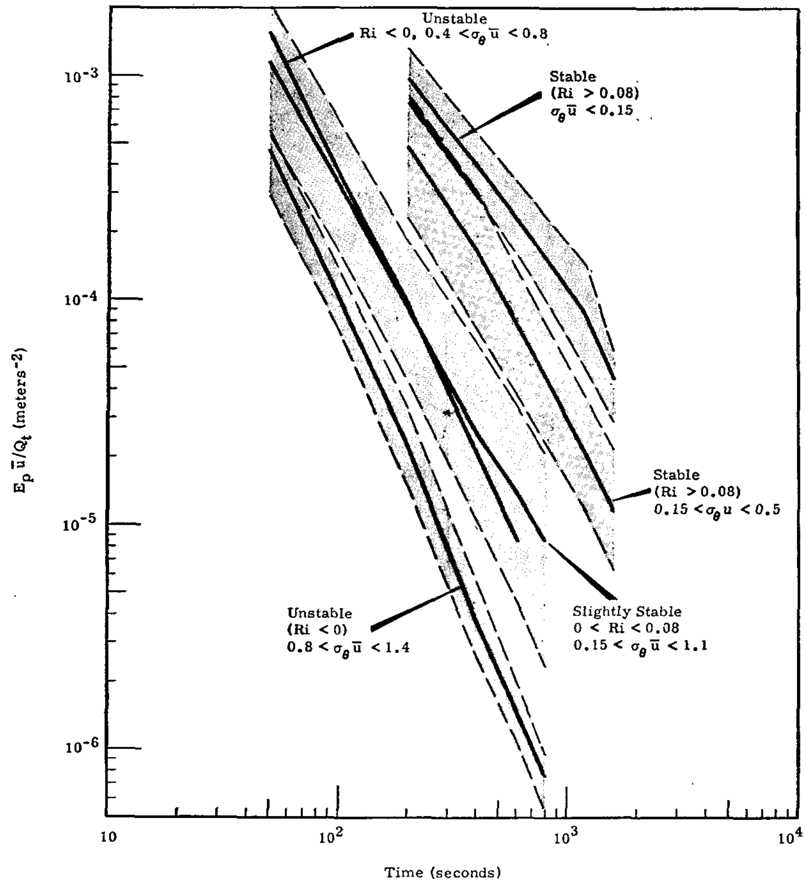

FIG. 7. Normalized peak exposure, $E_p\bar{u}/Q_T$, *vs.* time.

exposure distribution to be normal is valid. $\sigma_\theta\bar{u}$, Ri and $\bar{\theta}$ are calculated for each interval and the exposure distribution for each is determined from the graphs which have been presented. The final result is obtained by summing the individual solutions for the intervals. The composite is the exposure distribution which resulted from the actual release. This distribution may take any shape even through it was formed by summing curves which were normal.

7. Independent verification

Figs. 8, 9 and 10 show predicted exposure distributions for a stable run which was not used in developing the methods. The exposure is represented on the ordinate. The azimuth is given on the abscissa, the zero value selected to lie near the center of the distribution. The solid line connects the observed data. The dashed line is the predicted distribution which was derived through the summing of nine normal curves. The emission period for this run was three and one-half hours, much longer than any of the tests used to derive Figs. 5 or 7. Considering these complexities, the predictions of the positions and magnitudes of the major peaks are, indeed, encouraging, even at a distance of nearly 13 km (eight miles).

Fig. 11 compares predicted and observed values of the normalized exposures for eleven runs not included in developing the prediction methods. The comparison was made at 3200 meters from the source. Good verification has been obtained even through many of the runs were characterized by complex distributions. The circled data point represents a planned 40-minute run in which a trace quantity of elemental I^{131} was released near the ground. Prediction of the distribution began during the release and was completed shortly after its termination to test the adaptability of the procedures for applied problems.

8. Conclusions

The data definitely indicate that the crosswind variance of a plume is not a straightforward power function of time (or distance), but is proportional to the square of the travel time for times on the order of a few hundred seconds and proportional to the first power of time for times on the order of thousands of seconds. In addition, there is every indication that the standard

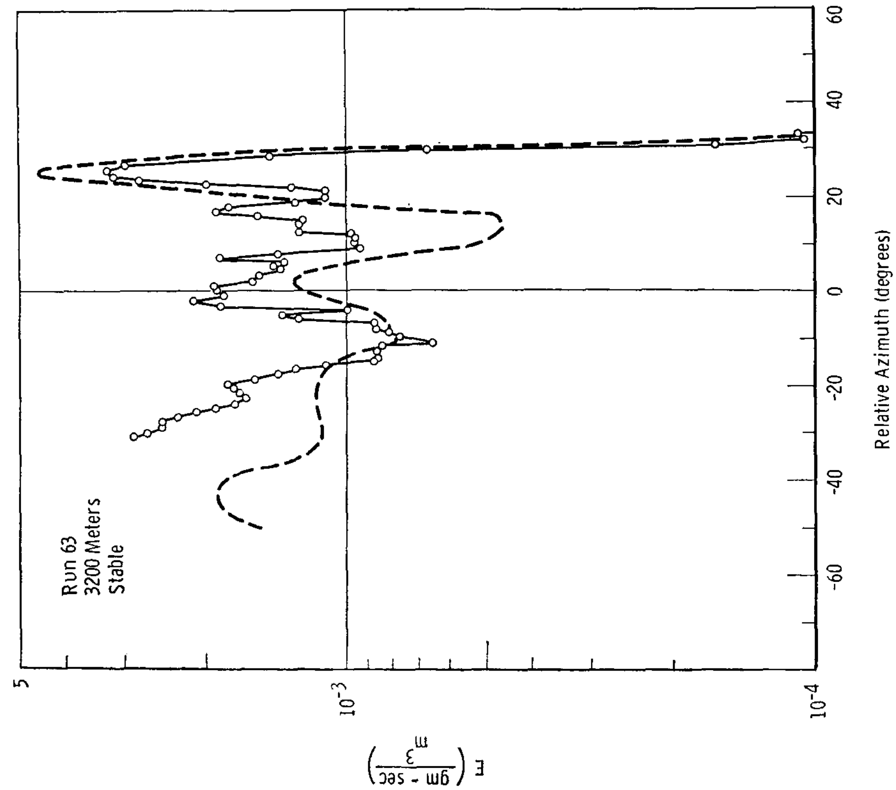

FIG. 9. Comparison of predicted and observed exposures.

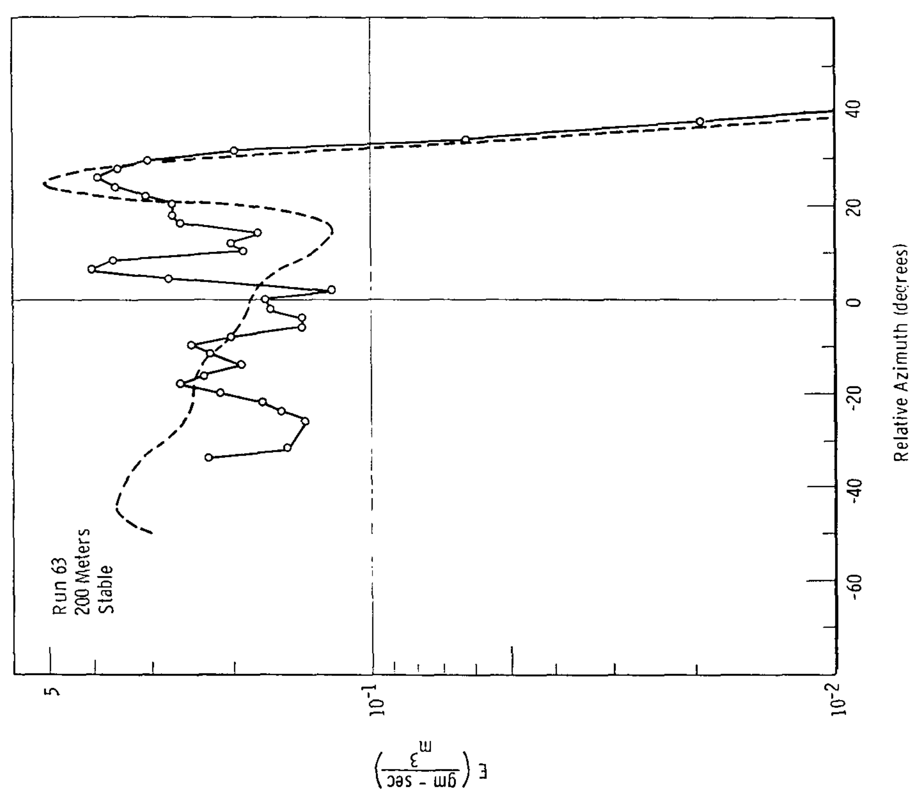

FIG. 8. Comparison of predicted and observed exposures.

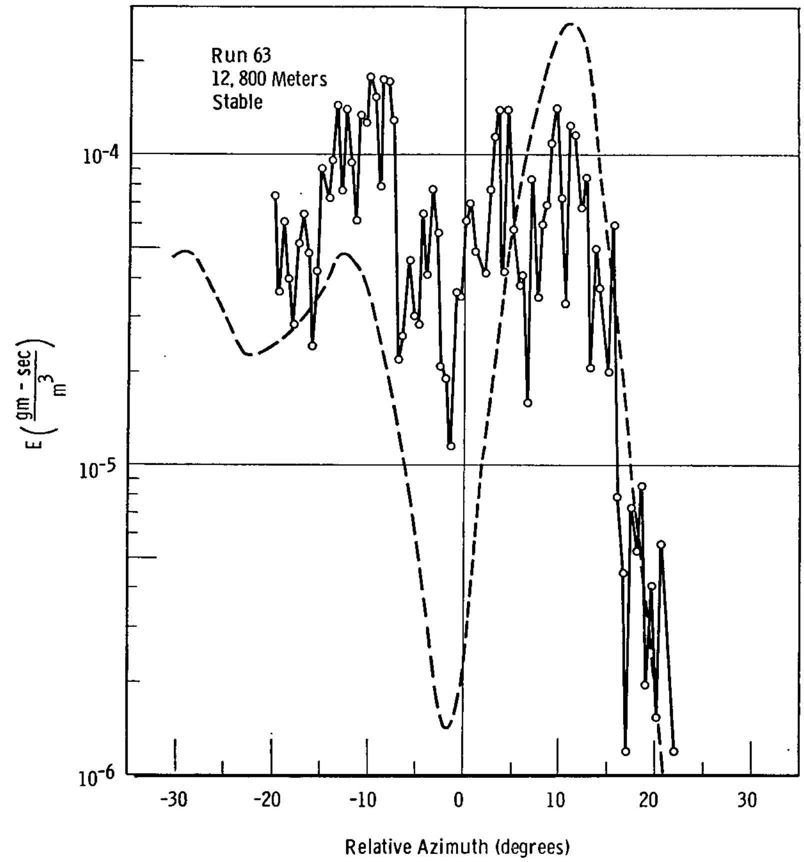

FIG. 10. Comparison of predicted and observed exposures

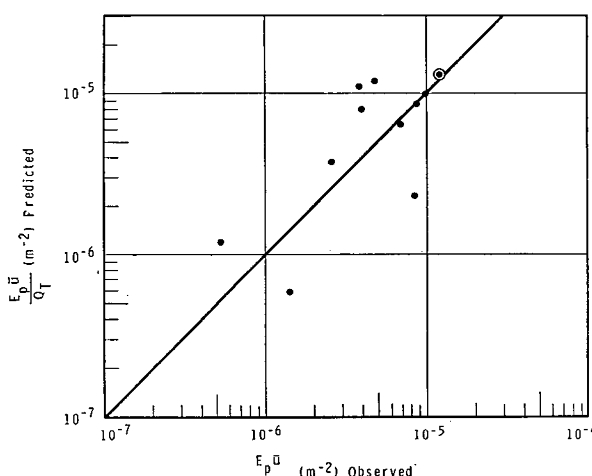

FIG. 11. Comparison of predicted and observed maximum exposures for 11 experiments at a distance of 3200 m.

deviation of wind direction, σ_θ, is not a parameter to use for discussion of crosswind diffusion; rather, the product $\sigma_\theta\bar{u}$, the Eulerian approximation to Lagrangian crosswind turbulent velocity, is to be used. These two results plus the concept of diffusion as a time dependent process, not distance dependent, yield a method for comparatively precise predictions of exposure distributions from sources near the ground.

Acknowledgments. The authors gratefully acknowledge the valuable suggestions made by Mr. J. W. Healy, of the General Electric Company.

REFERENCES

Barad, M. L., and J. J. Fuquay, 1962a: The Green Glow diffusion program, Vol. 1. *Geophysical Research Paper No. 73*, Geophysics Research Directorate, Air Force Cambridge Research Laboratory; Hanford Report HW 71400.

——, and ——, 1962b: The Green Glow diffusion program, Vol. II. *Geophysical Research Paper No. 73*, Geophysics Research Directorate, Air Force Cambridge Research Laboratory; Hanford Report HW-71400.

Lettau, H. H., 1957: Computation of Richardson numbers, classification of wind profiles and determination of roughness parameters. *Exploring the atmosphere's first mile*, Vol. I. New York, Pergamon Press, 376 pp.

Sutton, O. G., 1953: *Micrometeorology*. New York, McGraw-Hill, 333 pp.

Taylor, G. I., 1921: Diffusion by continuous movements. *Proceedings of the London Mathematical Society*, ser. 2, **20**, 196–211.